Monitoring Structural Deformation at Pacoima Dam, California Using Continuous GPS

Jeffrey A. Behr, *Southern California Earthquake Center, SCIGN-USGS*
Kenneth W. Hudnut and Nancy E. King, *United States Geological Survey*

BIOGRAPHY

Jeffrey A. Behr is Systems Specialist for the Southern California Integrated GPS Network (SCIGN). His present responsibilities include the development of software and systems for network communications, processing and analysis for the developing 250-station array, with emphasis on SCIGN's near-real-time earthquake response capability. He received his M. Sc. degree in Geological Sciences from the University of Colorado, Boulder, in 1992 and has been working in continuous GPS since 1993.

Kenneth W. Hudnut is a Geophysicist with the United States Geological Survey in Pasadena. He is a member of the SCIGN executive committee, vice chair of the SCIGN coordinating board and chairs the crustal deformation working group of the Southern California Earthquake Center. He received his Ph.D. in Geology from Columbia University in 1989.

Nancy King is a Geophysicist with the United States Geological Survey at USGS-Pasadena and is a member of the SCIGN Coordinating Board. She received her Ph.D. in Geophysics from the Scripps Institution of Oceanography in 1990.

ABSTRACT

Agencies responsible for dam safety have long used conventional surveying methods to measure the displacements of benchmarks as part of dam monitoring programs. Such surveys have provided infrequent though precise estimates of a dam's motions. With the development of high precision GPS methods to monitor plate tectonic motions and crustal deformation rates, an alternative method for monitoring such structural motions became available. While high- precision GPS approaches the horizontal positioning capability of conventional surveying methods, its great benefit lies in a much higher temporal resolution and nearly unattended continuous operation.

In September 1995, Pacoima Dam, located in the San Gabriel Mountains north of Los Angeles, California, was instrumented with a triad of continuously operating GPS receivers to test the feasibility of applying these techniques to the field of structural monitoring. Nearly three years of data have been analyzed from this sub-array to provide quarter-daily estimates of station-to-station baseline lengths. Quantitative methods were assessed to allow the identification of a number of outlying data points that could be misinterpreted as GPS station motion in a real-time system.

Figure 1. Pacoima Dam. Continuously recording GPS stations DAM1, on the left abutment, and DAM2 at the center of the arch are identified. View is to the north.

Examination of the derived baseline time series indicates that Pacoima Dam is experiencing an annual cycle of upstream-downstream (E-W) motion at the center of the dam arch of approximately 15-18 mm peak-to-peak

amplitude. Comparison of motion to daily regional temperature records strongly indicates that the dam responds to annual and shorter-period ambient temperature variations. Spectral methods are used to model this relationship to allow a more accurate estimation of the thermoelastic behavior of the structure.

INTRODUCTION

In coordination with the application of continuous GPS to crustal deformation monitoring in the L. A. Basin, the U. S. Geological Survey and Los Angeles County embarked in 1995 on an open-ended program to continuously monitor the positions of 2 points on Pacoima Dam, California (Figure 1). This structure (at 113 m, the tallest dam in the world at the time of its completion in 1929) experienced severe shaking (>1 g) and significant damage during the 1971 San Fernando and 1994 Northridge earthquakes (Swanson and Sharma, 1979; USGS and SCEC Scientists, 1994). On September 1, 1995, two monuments on the dam and another at the U. S. Forest Service's Fire Camp 9, 2.5 km to the NW (Figure 2), were instrumented with dual-frequency P-code GPS receivers and incorporated into the Los Angeles Basin's Dense GPS Geodetic Array. The design of this system, its communications and operations are based directly on that of the Permanent GPS Geodetic Array, the forerunner of SCIGN (Bock et al., 1997).

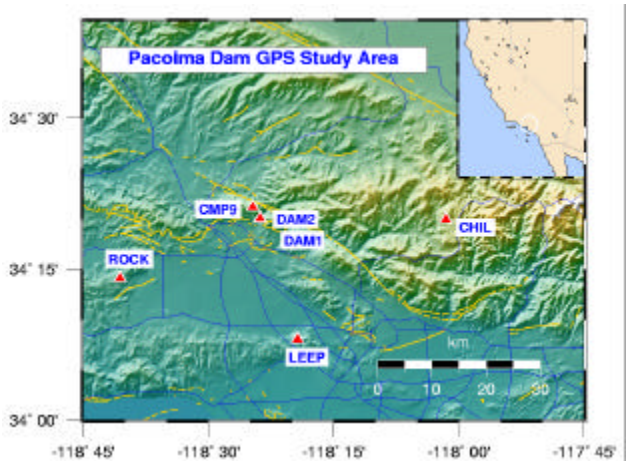

Figure 2. Location Map. In addition to stations DAM1 and DAM2, CMP9 station is less than 3 km away from Pacoima Dam. Data from three other SCIGN stations (ROCK, LEEP and CHIL) were also used in this study.

Pacoima Dam trends a few degrees west of north (abutment to abutment) in an east-west running section of steep-walled Pacoima Canyon. Station DAM1 was installed on the roof of a single-story, concrete operations building on the south (left) thrust block of the dam. Station DAM2 was installed near the center of the concrete arch atop a ~2 m tall steel-tube monument (Figure 3). These stations form a 103.7-m baseline differing in height by only 0.66 m. Station CMP9 sits atop a ridge approximately 2.5 km distant, more than 550 m above the dam's crest (Figure 2).

Hudnut and Behr (1998) describe the initial 2 years of operation and observations for this system. The highlight of that analysis was the identification of an oscillatory displacement of the DAM2 station of approximately 17-mm peak-to-peak amplitude with respect to DAM1 with an approximately annual period. The analysis showed that this displacement was strongly related to air temperature records from Burbank, CA., approximately 20 km to the south. It also suggested that the dam might be responding to higher frequency temperature variations. However, because the record available for that study was only two-years in length, we were only able to roughly estimate a transfer function between input temperature and output annual displacement. This paper reexamines this issue with the benefit of an added year of data. In addition, we reanalyzed the data in 6-hour sessions in order to assess the trade-off between decreasing latency and probable decrease in precision using higher-frequency GPS solutions.

Figure 3. Station DAM2. The Dorne-Margolin choke ring antenna is mounted on a steel pier, and GPS receiver, modem and power supply are in the NEMA-type enclosure mounted to the fencing.

A goal of earthquake response efforts is to obtain and provide rapid, accurate measurements of the locations and amplitudes of significant tilts, strains and displacements

following moderate to large earthquakes. At those same times and in much the same way, owners and operators of buildings and engineered structures need prompt, reliable estimates of structural displacements for safety and hazard analysis. But beyond this, continuously operating GPS, if implemented properly, can provide frequent, precise estimates of structural motions during periods unaffected by seismic motions.

GPS currently offers more than one method for structural monitoring applications. Two end-members of these methods might be described as static post-processing of GPS data (Hudnut & Behr, 1998) and Real-Time Kinematic (RTK) positioning (Celebi et al., 1998). While this paper summarizes our investigation of the first method, RTK methods are being tested at USGS-Pasadena for incorporation into the SCIGN as a supplemental tool for near-real-time earthquake displacement measurement. We have proposed and hope to implement real-time telemetry of RTK data from Pacoima Dam back to the USGS offices to aid the development of robust RTK systems for both structural monitoring and earthquake response.

GPS ANALYSIS

We performed quarter-day solutions for the Pacoima Dam network plus three additional SCIGN stations (ROCK, LEEP and CHIL) for 1059 days from September 1, 1995 to July 26, 1998. These solutions used phase and pseudorange data collected by Ashtech Z-12 dual-frequency, P-code receivers and choke-ring antennae. Precise ephemerides generated by the International GPS Service (IGS) (Beutler and Neilan, 1997) and UT1/polar motion estimates provided by the U.S. Naval Observatory (USNO) were used in the solutions.

We performed the initial processing of the GPS data using the GAMIT software (King and Bock, 1998). This package prepares the station observation data and IGS ephemeris, then computes the residual observations and partial derivatives from a geometric model. The package then marks and attempts to repair cycle-slips and outliers in the data using various combinations of phase and pseudorange data. Finally, station coordinates, orbital parameters and phase ambiguities are estimated in a least-squares adjustment.

Ambiguity resolution in GAMIT is an iterative process, involving the use of alternating estimations of geodetic parameters, real-valued, and integer biases using several combinations of phase and range data (Feigl et al., 1993). In short, geodetic parameters and real-valued biases are first estimated for all independent double differences using the ionosphere-free linear combination phase observable (LC). This is followed by estimation of wide-lane biases using independent L1 and L2 data while fixing the LC-derived geodetic parameters and applying appropriate constraints on the ionosphere. GAMIT next forces wide-lane biases to integer values using the decision-function (Dong and Bock, 1989) and the addition of P-code pseudo-range data. With wide-lanes now held fixed, geodetic parameters and L1 biases are estimated using the LC observations. After the narrow-lane (L1) biases are forced to integer values, again via the decision function, the LC observations are used once more for the final geodetic parameter estimation.

This set of geodetic parameters and corresponding variance-covariance matrices are next processed by the GLOBK Kalman filter adjustment software (Herring, 1998) to provide final quarter-daily estimates for the Pacoima Dam network. At this stage, we defined the reference frame for our analysis by applying *a priori* constraints of 5 ppb to the IGS orbits and 20 and 40 mm, respectively, to the horizontal and vertical coordinates of the two outermost stations of the network (CHIL and ROCK). These constraints are roughly twice the expected errors in these parameters (2-3 ppb for the orbits and 10-20 mm for the coordinates) (Table 1). Nonetheless, they are sufficiently tight that uncertainties in the orbits and the geocentric position of the network contribute less than 1 mm to the uncertainties of the unconstrained baselines in the analysis.

TABLE 1. *A priori* constraints applied in GLOBK.

Parameters	Constraints
Stations	20 mm NE, 40 mm Up - CHIL & ROCK
Satellites	0.10 m XYZ, 0.01 mm/s $V_x V_y V_z$
Pole	0.25 mas in XY, 0.1 mas/day
UT1	0.25 mas, 0.1 mas/day

GLOBK was developed to combine multiple loosely-constrained 'solutions' - estimates of geodetic parameters and their corresponding covariance matrices - in a single adjustment with uniform application of constraints. It is typically used to process global GPS data for the determination of satellite ephemerides, and regional data for the estimation of station velocities over multi-year spans. We use GLOBK primarily to perform a quality check on each independent solution. Poor-quality solutions are automatically rejected in the final adjustment. It also affords a computationally efficient method for testing various combinations of weights and constraints on the geodetic parameters derived from the GAMIT analysis. For example, once biases had been fixed in GAMIT, we were then able to process the data with varied constraints on the station coordinates to obtain an overall assessment of the quality of the bias-fixing.

PACOIMA DAM DATA

Following the GLOBK processing, we extracted baseline time series for stations CMP9, DAM1 and DAM2. The

time series were then demeaned and examined for jumps in the data due to site disturbances or equipment failures. Such jumps can strongly bias estimates of crustal velocities and are the subject of focused research in the SCIGN project. One such failure occurred at DAM2 when the original choke-ring antenna failed and was replaced on October 23, 1996 (662 days after January 1, 1995). The magnitude of this offset was estimated by linear least-squares fits to several multi-day spans of pre- and post-jump data from the CMP9-DAM2 and DAM1-DAM2 time series. The final adjustments and one-sigma uncertainties are summarized in Table 2. (Note that these are presented as baseline changes, not as absolute station positions.) Estimated uncertainties may be inflated due to a) a gap in the DAM1 time series shortly after the antenna was replaced, and b) our application of a linear fit to a time series with a significant oscillatory signal. Although there are more rigorous methods available to calculate these offsets, we did not consider them necessary for this analysis. It is apparent, however, that this adjustment provides some indication of the short-period detection threshold of the system in that we are able to observe horizontal displacements on the order of 4 mm on the 107-m baseline from DAM1-DAM2.

Table 2. DAM2 antenna change offsets in mm.

Baseline to:	North	East	Up	Length
CMP9 offset	-3.1	1.4	0.8	-1.6
CMP9 sigma	1.5	1.8	5.8	1.5
DAM1 offset	4.3	1.0	-1.8	4.3
DAM1 sigma	0.5	1.0	1.3	0.3

OUTLIER REJECTION

Not unexpectedly, the use of quarter-day solutions resulted in higher standard errors in the baseline estimates than daily processing, as well as several significant outliers in the time series. If the data were being examined as part of a real-time or near-real-time GPS system, these outliers might be interpreted as significant motion of the DAM2 station. For this reason, we attempt to identify parameters generated by the GAMIT/GLOBK processing that might be used to flag poor solutions.

During our initial analysis of two years' daily solutions (Hudnut & Behr, 1998) we suspected that the lack of data from one or more 'regional' GPS stations (ROCK, CHIL or LEEP) might weaken the quality of the network solution. We were concerned that the small aperture dam network would require distant sites to strengthen the network geometry. In that analysis all stations except DAM1 and DAM2 had coordinates constrained to 1-1-5 cm (NEU), while orbits and earth orientation parameters were loosely constrained. In essence, we were relying more on our regional station coordinates to define the reference frame. However, we found no relationship between missing regional data and outliers in the 24-hour solutions. Instead, we observed a relationship between low numbers of double difference observations and outlier occurrence.

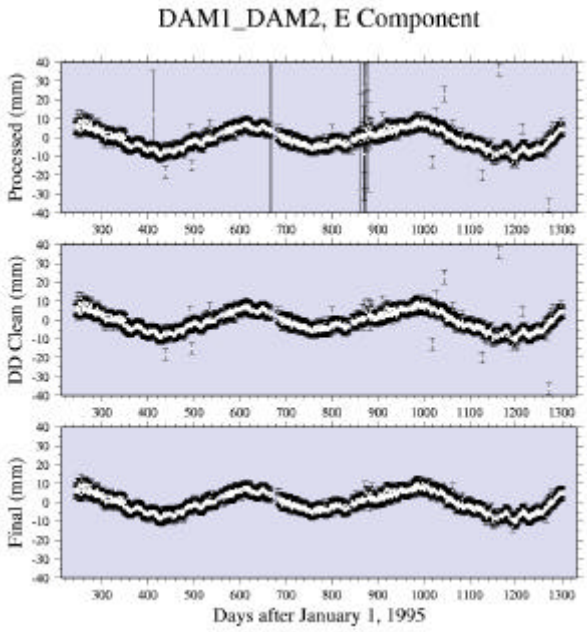

Figure 4. Outlier rejection results for the DAM1-DAM2 E-W baseline. Data extracted from the GAMIT/GLOBK solutions (top frame) have several extreme outliers removed via the double difference technique (middle). Little or no improvement was made in the application of the chi-square test so the remaining outliers were removed in a first-difference cut (bottom).

In the present treatment, our solutions have 75% fewer double differences because of the switch to quarter-day sessions while still processing at a 120-s sampling interval. Nevertheless, the low double-difference technique was again applied. We compiled 3-year time series of the number of double difference observations for each station for each 6-hour session and calculated mean values for each series. If either one of the baseline end-points provided less than 75% of mean values, we delete that session from all baseline time series involving that station. This succeeded in removing several outliers (Figure 4, Table 3) though it was less successful than its application to the 24-hour solutions.

We investigated a second rejection test by examining the values of the GLOBK chi-square per degree of freedom for each independent solution. As stated above, we use GLOBK to analyze each solution independently and to identify and reject sessions that exceed a configurable chi-square cutoff parameter, here set to 10.0. This cutoff may have been too high. Chi-square per degree of freedom should fall around 1.0 if the data have been weighted properly. We reexamined the GLOBK estimates and flagged solutions that had chi-square per degree of freedom > 3. Although 25 solutions were tagged and

removed, the Pacoima Dam time series cleaned by this method did not show significant decrease in the number of outliers. One probable failure with this technique is that the chi-square value is determined for all data in a solution and is not a site-specific parameter. This may lead to the rejection of high-quality data from the Pacoima Dam network when the problem data may have been from a regional station. At this point, we do not favor secondary removal of data based on high chi-square per degree of freedom.

Table 3. Baseline estimates after each cleaning stage.

Baseline	GAMIT/ GLOBK	Low DD	High Chi2	First Diff.	%
CMP9-DAM1	3911	3869	3847	3790	89
CMP9-DAM2	3893	3886	3862	3810	90
DAM1-DAM2	3831	3789	3767	3731	88

% is the total sessions out of a possible 4236 (1059 days, 4 sessions/day)

We have not yet found a satisfactory method for rigorous identification and removal of all outliers in the Pacoima Dam time series. Although the identification of low numbers of double differences holds promise for application in a near-real-time continuous GPS monitoring system, other methods for flagging poor quasi-observations need to be determined.

While systematic techniques for complete outlier removal have not been identified, in order to continue with the analysis of DAM2 motion we forced the removal of the remaining bad data. A first-difference (rate-of-change) time series was calculated for each component of the three baselines. The mean and standard deviation were then calculated for each component and all data points greater than 3-standard deviations from the mean were removed. Gaps in the time series were then filled using a linear interpolant (cubic and Akima splines were tested but introduced significant structure into the time series and were deemed inaccurate). This data set was used for the analysis of the deformation at Pacoima Dam.

The final, cleaned and adjusted DAM1-DAM2 time series are displayed in Figure 5. Although there is evidence that station DAM1 experiences annual displacement of a few mm opposite in trend to the motion of DAM2, we restrict our analysis to the dominant motion of the center of the dam arch. This is justifiable because of the lower uncertainties associated with the short DAM1-DAM2 baseline, and because of the existence of higher than average systematic noise in the data recorded at CMP9. This baseline focuses the deformation analysis along a segment of the dam that experienced troubling damage during the Northridge earthquake, extension and fracturing of the downstream façade at the left abutment/thrust block contact. Before analyzing recent deformation on this baseline, we examine the nature and the quality of the quarter-day baseline estimates.

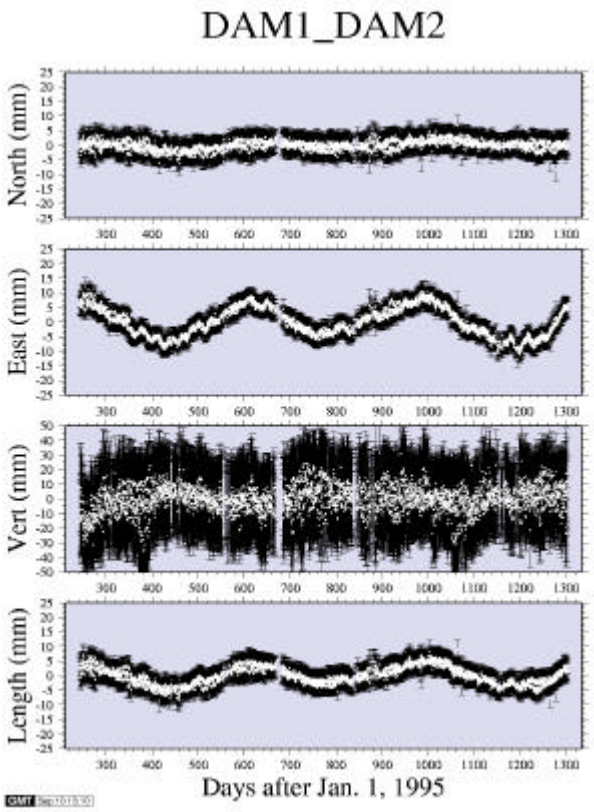

Figure 5. Final DAM1-DAM2 baseline time series, Sept. 1, 1995 through July 26, 1998. Time series have had outliers removed via double-difference, chi-square and first-difference techniques.

SUB-DAILY SOLUTIONS

During our analysis of the baseline time series power spectral density, we observed a surprising amount of power at the Nyquist frequency (2 cycles per day). It was an immediate concern that we were aliasing a high-frequency signal in the quarter-day solutions that had been averaged out in the daily solutions (Figure 6, frame 1). We observed in the E-W component of the DAM1-DAM2 quarter-day time series a repetitive displacement pattern in which the quarter-daily estimates varied by 2-3 mm from the daily position estimates. Aware of the thermoelastic response of the dam, we first looked for a correlation using sub-hourly temperature records from meteorological instruments located at SCIGN stations CHIL and CLAR (Chilao Flat in the San Gabriel Mts. and Claremont College in Claremont, CA.). However, no relationship could be found between sub-daily temperature and displacement because amplitude variations in the two signals did not correlate. We next examined baselines from the other sites in the network to determine if this was a site-specific effect and found that it was not.

The time series exhibit significant sub-daily scatter in the baseline lengths that appears to be systematic. In Figure 6 we display the E-W component of two baselines measured in the dam processing, DAM1-DAM2 and CHIL-LEEP, for a 20-day period from July 1997. This component is representative of the scatter in the north and length components, but approximately 25% of the amplitude in the vertical. The amplitude of the scatter in the CHIL-LEEP baseline is approximately twice that of DAM1-DAM2 while DAM1-DAM2 appears to be more repetitive in structure. These baselines differ in length by 2 orders-of-magnitude.

The structure in the baseline series reflects the scatter in the number of double differences available for each solution. Initial examination of short segments of double difference and position time series relate low number of double differences to the more extreme outliers. However, it is not yet clear if the low double differences reflect reduced satellite availability for these sessions or data cleaning, which might indicate a period of higher multipath for a particular session. It is clear that the dam stations have a myriad of multipath sources, but examination of phase residuals over several weeks and modeling of probable reflectors needs to be performed to assess a multipath source.

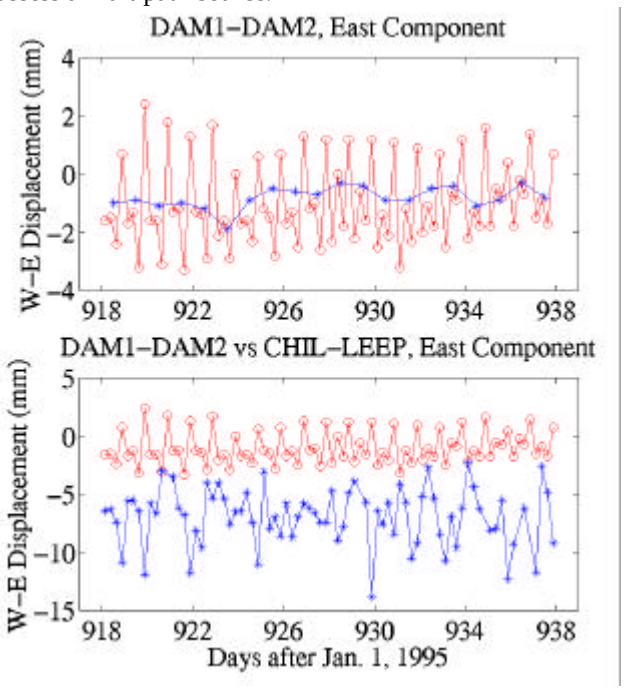

Figure 6. East component baseline length estimates for the DAM1-DAM2 and CHIL-LEEP baselines. DAM1-DAM2 quarter-day (o) vs. full-day (*) (frame 1) and CHIL-LEEP (*) (frame 2).

We have not yet begun to analyze the source of these signals, but have a number of possibilities to consider. They may be due to incorrectly resolved biases or a consequence of the fact that we do not use phase center models in our processing. They may be due to thermal effects on the receiver electronics, antenna LNA or antenna cable. It could possibly be azimuth and elevation dependent interactions with antenna radomes that would appear as phase noise similar to multipath. And it may be a combination of effects. In any case, now that this signal has been identified we can work to identify its source and methods to alleviate it, thereby improving the quality of sub-daily analyses and their applications.

THERMOELASTIC DEFORMATION AT DAM2

It was observed relatively early in the lifetime of the Pacoima Dam network that the dam was experiencing eastward displacement at the center of the concrete arch as regional temperatures increased, and westward displacement as temperatures cooled. Hudnut and Behr (1998) estimated a rough transfer function of 0.5 mm per degree F for the annual signals in these series, with a lag between nodes in temperature and displacement of about 40 days. We were not able to perform a rigorous analysis of the data using spectral methods because of the limited duration of the time series. In this analysis, however, we have available an additional year's data from Pacoima Dam and from the Burbank temperature sensor used in the previous study.

The Burbank temperature record is the nearest continuous data that we have for this analysis. Dam core temperature sensors were removed from the structure shortly after the Northridge earthquake and there are no continuous observations taken on the dam itself. Although we have now taken steps to alleviate this problem by installing a three-sensor meteorological package with the support of our colleagues in the SCIGN project, that sensor did not become operational until mid-August 1998. In the future we hope to be able to use the data from these on-site meteorological sensors to better estimate the thermal cycles in Pacoima Canyon. Additionally, although we processed the data in quarter-day solutions, we chose to analyze the coherence between the two signals using the daily temperature data and a displacement time series decimated to 1 sample per day using an anti-aliasing low-pass filter. As discussed in the previous section, we were unable to model short term variations in temperature and displacement due to the incoherence of the two signals recorded 10's of kilometers apart.

We present in Figure 7 the 3-year time series of Burbank temperature and DAM1-DAM2 E-W displacement. Our first step in the analysis of this data set was to detrend both time series by a sinusoidal signal of annual period to minimize the likelihood of low-frequency leakage into neighboring frequency bins. Although these series are not precisely fit by a sinusoid (note the advanced onset in spring 1997 and the retarded onset in spring 1998 of temperature increase and eastward displacement), this

approach was successful in removing much of the annual signal. Initial results using an impulse response function derived from input temperature and output displacement with annual signals present provided very poor results. Our results with the annual signal removed were much better. In removing the annual signal it was found that the best-fit sinusoids for displacement and temperature could be related by a gain of 1 mm per degree C with a lag of 35 days.

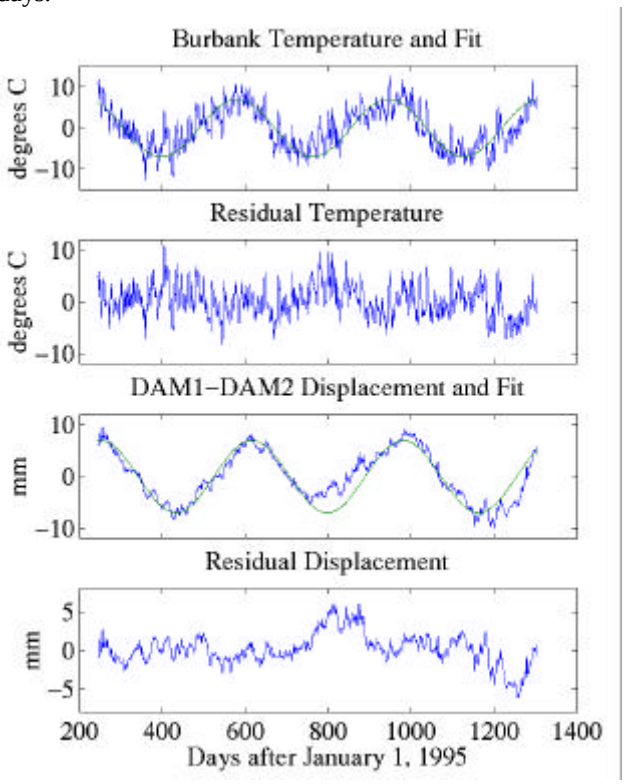

Figure 7. Three-year records of Burbank temperature and dam displacement fit by sinusoid function with annual period. The sinusoids are subtracted from the observed data to produce the residuals used in the spectral analysis.

We used Welch's method in MATLAB 5.1 to perform the spectral analysis. This method breaks the time series into shorter sections, estimates spectra for each section, and averages the results. This method reduces the variance of the estimated spectra, at the cost of reducing frequency resolution as well. To reduce bias (leakage) we applied a taper to each section. We used the Hanning taper and, after experimentation, a section length of 128 days.

We assume that temperature is the input to a linear time-invariant system with dam deformation as the output. In the time domain $y(t) = g(t)*x(t)$, where $x(t)$ is temperature, $y(t)$ is dam deformation, $g(t)$ is the impulse response function and * is the convolution operator. In the frequency domain $Y(\omega) = G(\omega)X(\omega)$ where ω is frequency and X, Y, and G are the Fourier transforms of x, y, and g, respectively. $G(\omega)$ is the complex-valued transfer function between the input and output describing the amplitude and phase changes as a function of frequency. For a linear system, the transfer function is $G(\omega)=h_{xy}(\omega)/h_{xx}(\omega)$, where $h_{xy}(\omega)$ is the cross-spectrum between input and output and $h_{xx}(\omega)$ is the power spectrum of the input. The gain spectrum, $|G(\omega)|$, and the phase spectrum, $\arg(G(\omega))$, describe how the system modifies amplitude and phase, respectively. Coherence $|h_{xy}(\omega)|^2/h_{xx}(\omega)h_{yy}(\omega)$ is in the range [0,1] and describes the correlation between input and output as a function of frequency. The impulse response function $g(t)$ is the inverse Fourier transform of the transfer function $G(\omega)$. Convolution of $g(t)$ with input temperature produces predicted output and allows us to assess the success of the model. See Priestley (1981) for a complete description of these methods.

The coherence, gain and phase calculated for input residual temperature and output residual displacement are presented in Figure 8. The series appear to be coherent up to a frequency of approximately 1 cycle per 14 days. Beyond that frequency our confidence in the estimated transfer function is limited. We find that the gain falls off at $1/f^2$ and our phase lag is fairly constant between −35 and -50 degrees.

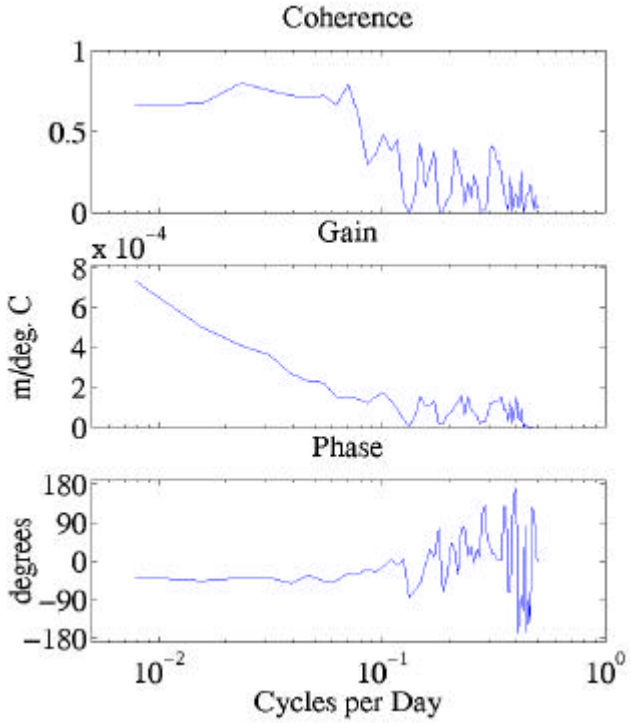

Figure 8. Coherence, gain and phase between input Burbank temperature and output dam displacement. Analysis performed with a data section length of 128 days.

The application of the impulse response function obtained from this transfer function provides a reasonable fit to the displacement data (Figure 9). Input temperature (frame 1) is convolved with the impulse response function

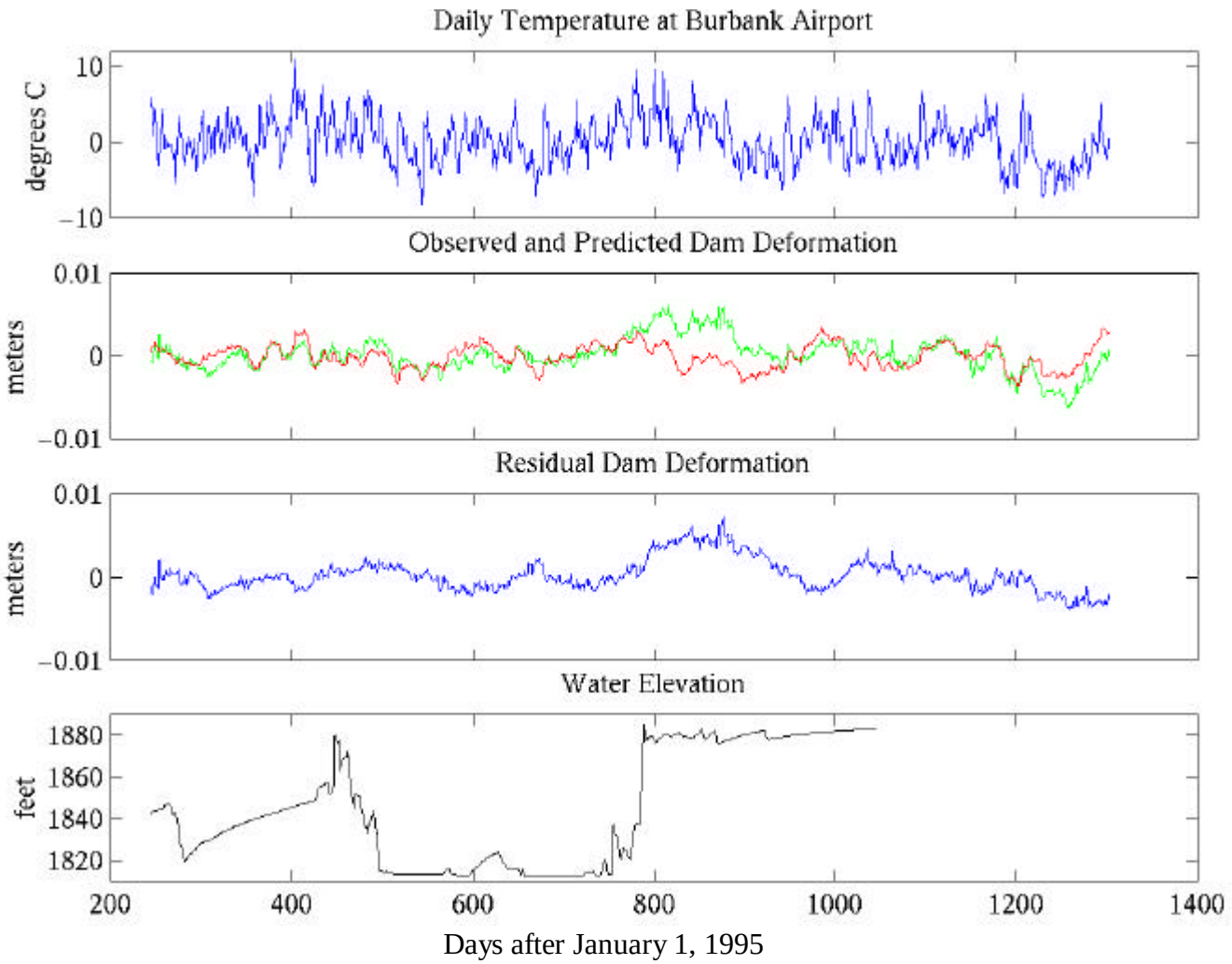

Figure 9. Convolution of the derived impulse response function with temperature from the Burbank Valley pumping station, September 1, 1995 through July 26, 1998. The filter was convolved with temperature data with the annual signal removed (frame 1) to produce a time series of predicted deformation (dark/red trace, frame 2) which compares reasonably well to observed deformation (light/green trace, frame 2). The predicted deformation is then subtracted from the observed deformation to produce a time series of residual deformation (frame 3) with thermoelastic signal removed. Displacements remaining in this series show clear evidence for a relationship between dam displacement and periods of increased reservoir depth (frame 4) at Pacoima Dam.

to create a time series of predicted dam displacements (frame 2). When this predicted series is subtracted from the observed dam deformation we are left with a residual time series of dam deformation (frame 3) with thermally-induced displacements removed. The signal remaining in the residual time series show much less strength for periods of a few to several days out to a few weeks. One of the strongest signals in the residual series may be a response to a rapid increase in reservoir elevation at ~780-790 days after Jan. 1, 1995.

Although the coherence estimate between temperature and displacement was not significantly strong at periods shorter than 2 weeks, there are some significant variations in the predicted deformation that correspond with observed displacements totaling a few mm over periods of a few to several days. While the largest signals occur over periods of a few weeks, the impulse response function seems to have predicted some short-term displacements. The residual deformation record shows an overall reduction in displacements of more than 1-3 mm over periods of a few days to a few weeks.

While a simple physical model might easily be developed for this system, one was not attempted here due to limitations in time. However, the gain, which appears to fall off as $1/f^2$ from a value of 1mm/°C at annual period, corresponds well to a coefficient of thermal expansion of

10^{-5}/°C, a typical value for steel and concrete. For a structure of 113-m height and approximately 150-m arch length, this would result in a thermoelastic coefficient of ~10^{-3}/°C, essentially what we observe on this dam. The other factor would be the coefficient of thermal diffusivity controlling the rate at which the dam absorbs heat into its core.

CONCLUSIONS

At this time our evaluation of the dam at daily or sub-daily intervals is limited due to our discovery of systematic noise in the sub-daily GPS positions. We will pursue identification and reduction of this noise as a way of further reducing latency while maintaining accurate, absolute positions. Our goal is to improve on a current horizontal resolution of 4-6 mm each day, as is done typically for SCIGN near-real-time analysis at USGS-Pasadena (http://www-socal.wr.usgs.gov/scign/Analysis).

The Pacoima Dam experiment successfully demonstrates the applicability of continuous GPS to the field of structural monitoring. The 3-year DAM1 to DAM2 baseline time series indicates that the center of the dam arch undergoes an annual cycle of E-W displacement with peak-to-peak amplitude of 17±2 mm. Conventional surveying measurements taken after the 1994 Northridge and the 1971 San Fernando earthquakes indicate that the arch of the dam moved eastward by approximately 0.5 and 0.6 inches, respectively (Morrison Knudsen Corp., 1994). These displacements are within the range of thermoelastic signals reported here. It is unclear whether or not the earthquake-related measurements accounted for thermally induced displacement.

Spectral analysis of the residual time series (annual cycle removed) indicates strong coherence at frequencies as high as 1 cycle per 14 days between remotely recorded temperature and dam displacement. We were able to derive and apply an impulse response function between input temperature and output displacement that enable a resolution of 2-4 mm displacement over periods of a few days. The residual deformation record could be used to model the structure's response to changes in reservoir level and to identify anomalous displacements at Pacoima Dam.

ACKNOWLEDGEMENTS

This project would not have been possible without the efforts of Bob Reader, Robert Kroll and Chuck Peer at L.A. County Department of Public Works. Much the same can be said for our colleagues in SCIGN and the IGS for the infrastructure they provide. We thank Maryann Vander Vis, also of L.A. County D.P.W., for compiling geotechnical data from, and background research on, Pacoima Dam. Repeated thanks are due to John Galetzka, Aris Aspiotes, Shannon Van Wyk and Daryl Baisley at USGS-SCIGN Operations Center and to L.A. County dam personnel for the installation and continued excellent operation of the GPS stations. Special thanks go to Robert King for his review of a draft of this paper and his continued guidance in GPS data analysis, and to Hadley Johnson and Duncan Agnew for their insights and suggestions on time series analysis techniques. The photographs in Figures 1 and 3 were taken by John Galetzka.

REFERENCES

Beutler, G., and R. Neilan (1997). International GPS Service for Geodynamics, International Association of Geodesy General Assembly, Rio de Janeiro, Brazil, September 3-9, 1997.

Bock, Y., S. Wdowinski, P. Fang, J. Zhang, S. Williams, H. Johnson, J. Behr, J. Gengrich, J. Dean, M. van Domselaar, D. Agnew, F. Wyatt, K. Stark, B. Oral, K. Hudnut, R. King, T. Herring, S. Dinardo, W. Young, D. Jackson and W. Gurtner (1997). Southern California permanent GPS geodetic array: continuous measurements of regional crustal deformation between the 1992 Landers and 1994 Northridge earthquakes, *J. Geophys. Res.*, **102**, B8, pp. 18013-18033.

Celebi, M., W. Prescott, R. Stein, K. Hudnut, J. Behr and S. Wilson (1998). GPS Monitoring of structures: recent advances, submitted to *Earthquake Spectra*.

Dong, D.-N., and Y. Bock (1989). Global Positioning System network analysis with phase ambiguity resolution applied to crustal deformation studies in California, *Journal of Geophysical Research*, **94**, pp. 3949-3966.

Feigl, K., D. C. Agnew, Y. Bock, D.-N. Dong, A. Donnellan, B. H. Hager, T. A. Herring, D. D. Jackson, R. W. King, S. K. Larsen, K. M. Larson, M. H. Murray, Z.-K. Shen (1993). Measurement of the velocity field in central and southern California, *Journal of Geophysical Research*, **98**, pp. 21667-21712.

Herring, T. A. (1998). GLOBK: Global Kalman Filter VLBI and GPS analysis program, Mass. Inst. Of Technol., Cambridge.

Hudnut, K. W. and J. A. Behr (1998). Continuous GPS monitoring of structural deformation at Pacoima Dam, California, *Seismological Research Letters*, **69**, No. 4, pp. 299-308.

Hudnut, K. (1996). Continuous GPS monitoring of dam deformation. *EOS, Trans. AGU*, **77**, No. 46, p. F139.

Hudnut, K. W., Z. Shen, M. Murray, S. McClusky, R. King, T. Herring, B. Hager, Y. Feng, P. Fang, A. Donnellan, and Y. Bock (1996). Coseismic displacements of the 1994 Northridge, Calif., earthquake, *Bull. Seis. Soc. Amer*. (Special Issue), **86**, No. 1, Part B, pp. S19-S36.

King, R. W. and Y. Bock (1998). Documentation for the MIT GPS analysis software: GAMIT, Mass. Inst. of Technol., Cambridge.

Morrison Knudsen Corporation (1994). Report on initial assessment of the effects of the January 17, 1994 Northridge/San Fernando earthquake on Pacoima Dam, Phase 1, County of Los Angeles Dept. of Public Works.

Priestley, M.B. (1981). Spectral Analysis and Time Series, Academic Press, London.

Swanson, A. A. and R. P. Sharma (1979). Effects of the 1971 San Fernando earthquake on Pacoima Arch Dam, *International Commission of Large Dams, Proceedings*; New Delhi, India, pp. 797-824.

USGS and SCEC Scientists (1994). The magnitude 6.7 Northridge, California earthquake of January 17, 1994, *Science*, **266**, pp. 389-397.